OPTIMIZATION OF FAST THREE-ELECTRODE SPARK GAPS ISOLATED WITH A SF6 AND He MIXTURE

by

Teodora M. NEDIĆ [1], ***Djordje R. LAZAREVIĆ*** [2],
Koviljka D. STANKOVIĆ [2], ***and Nenad M. KARTALOVIĆ*** [3]

[1] Faculty of Technology and Metallurgy, University of Belgrade, Belgrade, Serbia
[2] Faculty of Electrical Engineering, University of Belgrade, Belgrade, Serbia
[3] Institute of Electrical Engineering "Nikola Tesla", Belgrade, Serbia

Scientific paper
https://doi.org/10.2298/NTRP2103234N

This paper considered the possibility of reducing the dissipation of the trigger time of the three-electrode spark gaps with a separated triggered electrode. The work is of a theoretical, numerical and of experimental nature. The experiments were performed on a spark gap model under well-controlled laboratory conditions. It was determined that the results obtained with the model can be applied to the spark gap prototype. Unlike the previous research in this area, the computer-designed spark gap that was used can be triggered with one mechanism only. Also, as opposed to the previous study, a mixture of SF_6 and He gases and the third electrode with a double ionization effect were used. The obtained results showed the optimal combination of the construction solution, insulation gas, triggered impulse, and the triggered electrode's shape, reduce the stochastic dissipation of a random variable far in the sub-microsecond field. This result is of great significance for the parallel triggering of current and voltage generators to obtain the best superposition signals.

Key words: three-electrode spark gap, statistical dissipation of the trigger time, the mixture of SF_6 and He gases

INTRODUCTION

A synthetic circuit for testing high power switches, an energy injecting system into nuclear fusion plasma, parallel operation of voltage or current impulse generators, *etc*., can only be achieved by high-synchronization trigger switches [1, 2]. Such switches must not be exposed to stochastic processes, *i. e*. when determining their parameters, the measurement uncertainty type A should be zero (or approximately zero) [3, 4].

The spark switches have been used to achieve these overly demanding conditions [5, 6]. The functioning of the spark switches is based on bringing the external energy with a two-electrode system isolated with reversible dielectrics, thus causing the breakdown. In this way, the spark switch becomes *controlled*.

The control of the spark switch is performed with a computer system, which, in addition to the spark switch, controls and co-ordinates the whole series of the system parameters in which the switch is installed [7, 8].

There are two controlled spark gaps triggered methods: 1 – usage of an additional (third) electrode and 2 – laser injection of the energy into the electrode space [9-11]. Since the usage of a third-electrode has shown a satisfactory degree of synchronization and controllability with easier fitting into the control system and certainly a lower price, it is more commonly used [12-14].

This paper examined and compared the methods for minimizing the statistical dissipation of the trigger time or minimizing the jitter, for the superposition of signals from the simultaneously triggered generators.

THE TRIGGERING MECHANISM FOR THE THREE-ELECTRODE SPARK GAPS

The choice of the three-electrode spark gaps type is reduced to the position choices of the triggered electrode. Specifically, the construction solution of the three-electrode spark gaps can be performed with a triggered electrode separated from the main electrodes, fig. 1(a) and a triggered electrode inside one of the main electrodes, fig. 1(b). This paper examined the characteristics and principles of functioning, a type of three-electrode spark gap with a separated triggered electrode from the main electrodes.

* Corresponding author; e-mail: teodora.nedic@nuklearniobjekti.rs

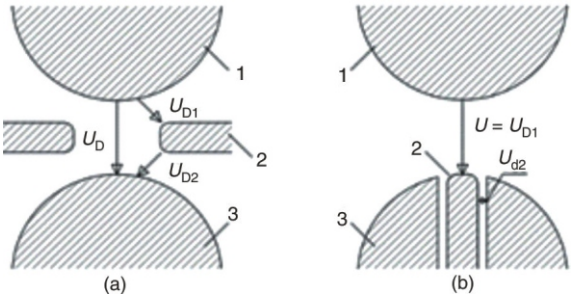

Figure 1. The three-electrode spark gap: (a) the triggered electrode outside the main electrode and (b) the triggered electrode in the main electrode

In order to explain the mechanism of operation of this spark gap type, it will be assumed that one of the main electrodes is located at a positive potential (high voltage main electrode) and the other one is grounded (grounded main electrode). The third, triggered electrode, in this case, should be placed at the potential of the equipotential line on which it is located (easily achieved by an ohmic voltage divider).

The triggering of such a three-electrode spark gap is realized by bringing a negative impulse to the trigger (third) electrode. Three breakdown mechanisms are then possible depending on the rations of voltage U_R, U_{D1}, and U_{D2} shown in fig. 1.

If $U_R > U_{D2}$, after triggering the third (triggered) electrode, in some time t, it will reach the value of U_{D1}. This creates a condition for a breakdown between the main high voltage electrode and the triggered electrode. This breakdown leads to an increase in the voltage of the trigger electrode. When the triggered electrode reaches the value of U_{D2}, after some time t, the breakdown occurs between it and the main grounded electrode. This terminates the spark gap breakdown. Time, t, is the time required to form a spark [15]. Figure 2(a) shows the process of this breakdown mechanism (Mechanism I).

If $U_R < U_{D2}$, after triggering the third (triggered) electrode, for some time, t, it will reach the value of U_R. This creates a condition for the breakdown between the main high voltage electrode and the triggered electrode. The triggered electrode is retained at the UR voltage until

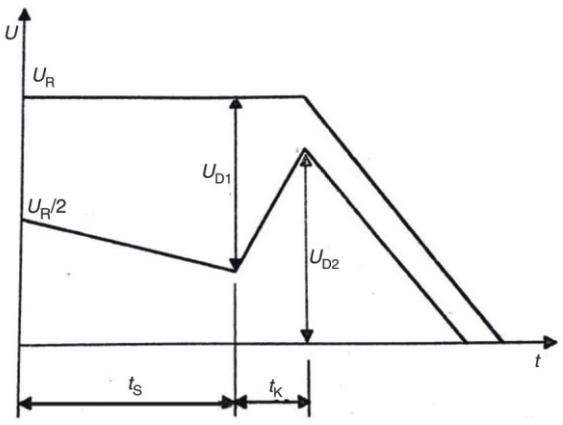

Figure 2(a). The trigger Mechanism I

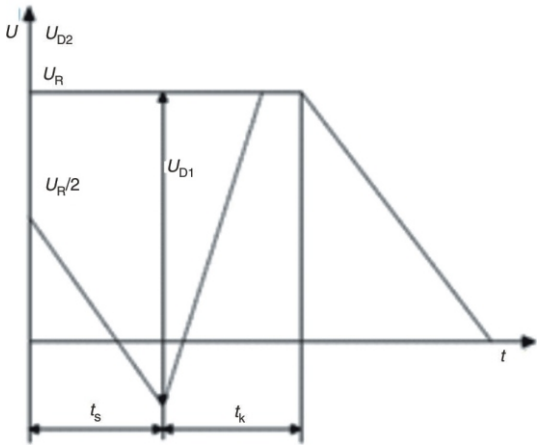

Figure 2(b). The trigger Mechanism II

the breakdown voltage between the triggered electrode and the main grounded electrode does not drop to the U_R value due to the photoionization induced by the previous breakdown. At that point, the breakdown occurs between the main electrodes. This terminates the spark gap breakdown. Figure 2(b) shows the process of this breakdown mechanism (Mechanism II).

If U_{D1} U_{D2}, the triggering of the three-electrode spark gaps will be possible only if the triggered electrode is not located in the middle between the main electrodes, otherwise, the breakdown occurs first between the main grounded electrode and the triggered electrode. In this case, after triggering the third (triggered) electrode, after some time, t, a breakdown occurs between the main grounded electrode and the triggered electrode. After the breakdown between these two electrodes, the triggered electrode has a grounded potential. As in the previous case, this breakdown leads to photoionization, which reduces the breakdown voltage value between the triggered electrode and the main high voltage electrode. At that point, a breakdown occurs between the main electrodes. This terminates the spark gap breakdown. Figure 2(c) shows the process of this breakdown mechanism (Mechanism III).

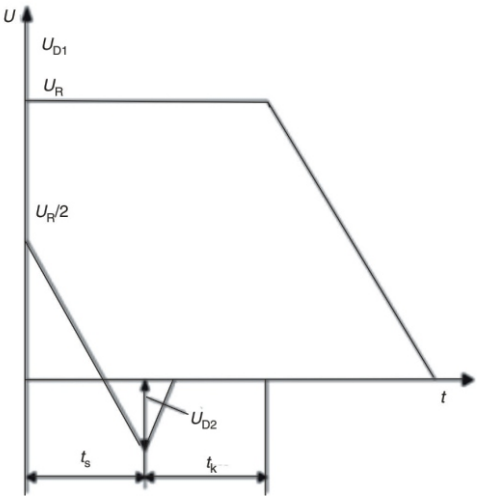

Figure 2(c). The trigger Mechanism III

Since the triggering, in all three described mechanisms, is performed by impulse voltage of the trigger voltage value and the trigger time, these are stochastic magnitudes [16]. In the case of Mechanism I, which is the least stochastic as, in that case, the spark triggering does not depend on the stochastic occurrence of electrical discharge in the interelectrode space as a consequence of the first breakdown step [17, 18].

A measure of the quality of the three-electrode spark gaps is the statistical dissipation of the trigger time. The smaller it is, the greater the spark gap. This is important because the spark gap during the application should perform the triggering at the right time. This is particularly pronounced when multiple identical spark gaps simultaneously perform the triggering by multiple parallel-coupled voltage (or current) generators in order to substitute sub-microsecond width output signals with minimal jitter (in high energy physical experiments) [19, 20]. For this purpose, it is advisable to use a spark gap in which the triggering is performed by Mechanism I (for the reasons stated above).

The trigger time of the three-electrode spark gaps, t_t is the expiring time from the moment of bringing the impulse voltage to the triggered electrode until the moment of the spark gap breakdown-ends. The components of the trigger time Mechanisms I are: 1 – dc time, t_{DC} (the expired time from bringing the impulse voltage to the triggered electrode to achieving a potential difference between the triggered electrode and main high voltage electrode equal to the dc breakdown voltage value of that interelectrode gap); 2 – statistical time, t_s (the expired time from the appearance of a free electron in the space volume, the so-called critical volume, within which a free electron can absorb enough energy at one medium of the free path from the electric field to perform ionization and thus become an initial electron), 3 – the time of avalanche formation t_l (the expired time from the formation of the first avalanche and terminates terminated by bridging the interelectrode space with the first streamer), and 4 – the formative time, t_f (the expired time from the thermo-ionization beginning of the streamer to the end of the breakdown) [21-24]. Figure 3 shows the components of the trigger time.

As the triggering of a three-electrode spark gaps consists of two approximately symmetrical steps, it can be shown by the eq. (1)

$$t_t \quad t_{DC} \quad 2t_s \quad 2t_\ell \quad 2t_f \qquad (1)$$

In eq. (1) all magnitudes are stochastic, so the trigger time is also stochastic.

To the statistical nature trigger time contributes the most to the and at least to the (which for a constant form of the trigger impulse is almost a deterministic magnitude). The times and are stochastic magnitudes with less pronounced statistical dissipation than the time [25-27].

Considering the previous explanation, it can be concluded that to optimize the characteristics of the three-electrode spark gaps, the following is required: 1 – construct the three-electrode spark gaps which are 100 % triggered by Mechanism I, and 2 – minimize the statistical dissipation of the trigger time by selecting the trigger impulse shape, electrode processing, choosing the material of the electrode and the insulating gas [28-30].

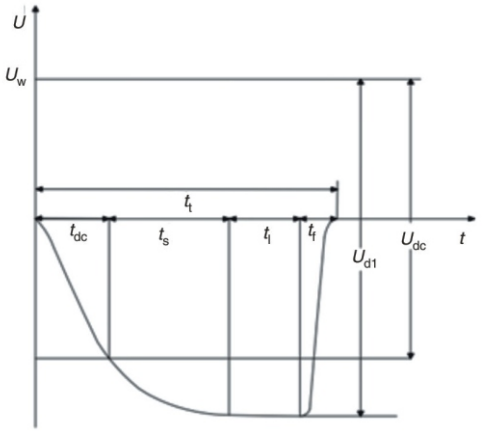

Figure 3. The trigger process by Mechanism I and components of the trigger time

COMPUTER DESIGN OF THREE-ELECTRODE SPARK GAPS

The initial phase for the computer design of the three-electrode spark gaps triggered by the Mechanism I is the basic form of the three-electrode spark gaps with the triggered electrode midway between the main electrodes, fig. 4 (*i. e.* with the standard triggered electrode). The calculation parameters were: the radius of the main electrodes, *R*, the interelectrode distance, *d*, the diameter of the central cavity of the triggered electrode, , the thickness of the third electrode, *e*, and the radius of curvature of the edge of the third electrode, *r*.

The electric field in the interelectrode space was calculated by the charge simulation method. The num-

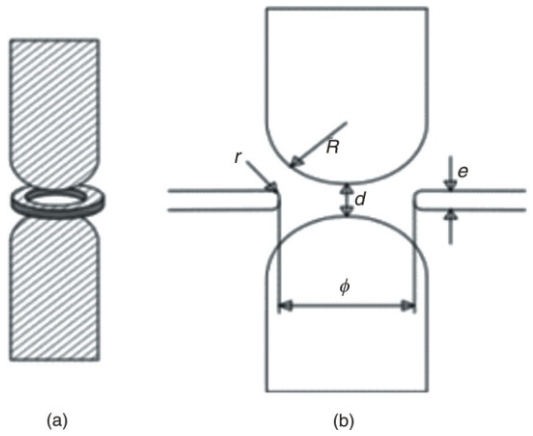

Figure 4. The general form of a three-electrode spark gap for triggering by Mechanism I: (a) the standard form and (b) the parameters for calculation

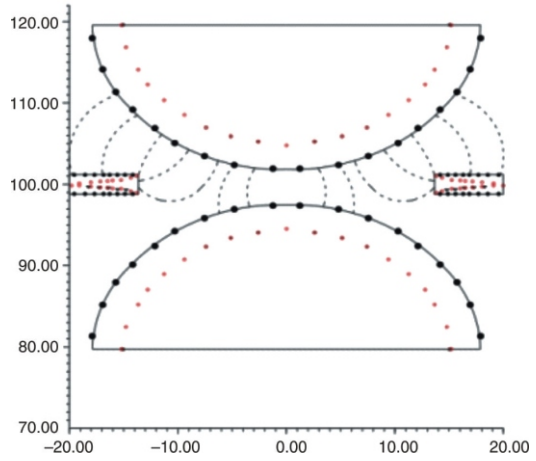

Figure 5. The calculation of spark gap dimensions for triggering by Mechanism I; · fictitious charges, checkpoints, ···· field lines

ber of contour and control points were set automatically depending on the desired accuracy (which was high). Figure 5 shows an example of an electric field calculation described by a three-electrode spark gap method that accomplished the trigger requirement by the Mechanism I [31-33].

Following the calculation of the electric field, the breakdown voltage was calculated according to the condition for the streamer breakdown mechanism, as, according to the product value pd (gas pressure x interelectrode distance in the spark gap), only this mechanism could be expected [34, 35]. Tausend's coefficients for the applied gases and gas mixtures were determined based on the assumption of Maxwell's free-electron gas distribution [36].

EXPERIMENT AND PROCESSING OF EXPERIMENTAL RESULTS

The idea of the experiment was to determine the influence exerted on the statistical dissipation of the trigger time of the numerically designed spark gap in the unstable equilibrium (*i. e.* at a voltage between the main electrodes 5 % lower than the spontaneous breakdown voltage) of the following parameters: 1 – composition of the working gas mixture $SF_6 + (1 - x)$ He, 2 – shape of the trigger impulse, and 3 – shape of the inner edge of the triggered electrode.

For the purpose of this experiment, a flexible model of optimal dimensions determined by the numerical procedure (R = 18 mm, d = 0.55 mm, Ø = 0.25 mm, e = 2.5 mm, and r = 0.25 mm) was made, fig. 6. The small dimensions of the spark gaps model made it possible to experiment with spark gap characteristics that could not be captured by the computer design procedure. The results obtained on the spark gap model could, under the law of similarity, be transmitted to the prototype and the final product of the spark gap [37]. Such a procedure, *i. e.* suitably reduced spark gap

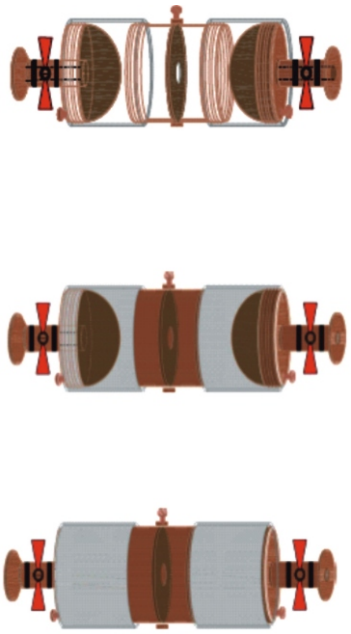

Figure 6. The flexible experimental model of the three-electrode spark gap

model, simplifies the experiment, and the results obtained provide reliable guidance for the further construction of the final spark gaps.

The spark gap model is connected to the gas circuit, after multiple vacuuming and rinsing with SF6 gas, filled with a gas mixture SF6 + (1 – x) He of the desired composition and pressure (*i. e.* 5 % less than the spontaneously triggered pressure determined numerically and experimentally). The composition of the mixture was determined according to the law of additive (partial) pressures [38, 39]. During the experiment, the percentage of the SF6 gas in the mixture was: 90 %, 80 %, 70 %, and 60 %. Figure 7 shows the gas circuit for the vacuum and the model of the three-electrode spark gaps gas filled.

Figure 8 shows the circuit for the trigger time measuring. The circuit for triggering of the three-electrode spark gaps in the circuit shown in fig. 8 had a DC output (DC voltage rise rate of 8 Vs^{-1}) and linear im-

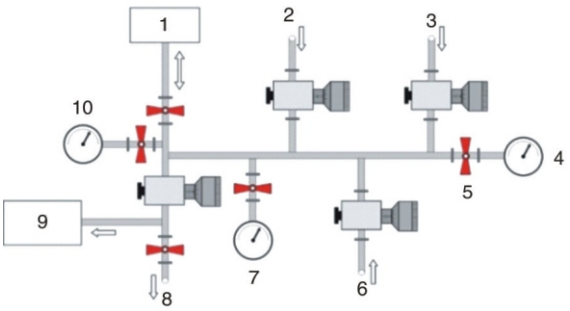

Figure 7. The main system for filling the three-electrode spark gaps with the gas mixture; *1 – chamber, 2 – SF6 gas, 3 – He gas, 4 – vacuum gauge, 5 – two position valve, 6 – air, 7 – manometer, 8 – irradiation, 9 – vacuum pump, and 10 – precision vacuum*

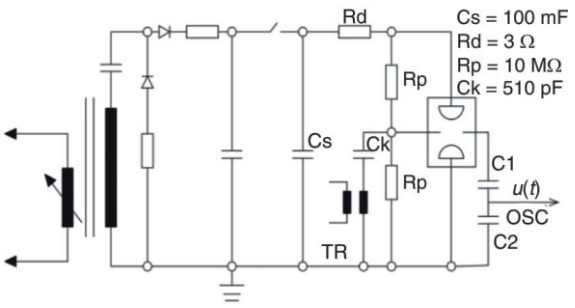

Figure 8. The circuit for trigger time measuring

pulse output (for impulse rise rate 1 kV(μs)$^{-1}$, 5 kV(μs)$^{-1}$, 10 kV(μs)$^{-1}$, 20 kV(μs)$^{-1}$, 50 kV(μs)$^{-1}$, and 100 kV(μs)$^{-1}$. The impulse voltages were the double-exponential amplitude type, significantly larger than the breakdown voltage value. The trigger time was measured by a fast nanosecond compensated capacitive divider [40]. During the measurement, the measuring and control instruments were placed in a 100 dB protection cabin that was galvanically separated from the measuring circuit. The experiments were performed under well-controlled laboratory conditions. The combined measurement uncertainty was less than 5 % [41-43].

The SF_6 insulation gas is very commonly used in electroenergetics. The usage of this gas has prevailed because of its good insulation characteristics as a result of its electronegativity, as well as other properties. The use of SF_6 gas enables a significant reduction in the dimensions of individual electroenergetic components. Accordingly, the SF_6 is the basic insulation gas in the three-electrode spark gaps. However, with the gas tendency to generate negative ions, it reduces the number of free electrons and significantly extends the statistical time (and thus its stochastic dissipation). The SF_6 gas also prolongs the formative time and its statistical dissipation as the large SF_6 molecule by its inertia slows down the thermo-ionization process. To reduce these two effects that increase the statistical dissipation of the trigger time, the three-electrode spark gaps were isolated by a gas mixture of SF_6 and He. The He is a monoatomic gas of extremely low ionization energy (it releases electrons easily), of low mass, *i. e.* high mobility and no vibrational and rotational quantum mechanical states. These properties create a positive synergistic effect in the three-electrode spark gaps in the SF_6 gas mixture. Namely, its easy release of electrons compensates for the loss of electrons due to their capture by the electronegative SF_6 gas and thus prevents the increase of statistical time. The mobility of helium ions accelerates the heat transfer in the strimmer and significantly shortens the thermo-ionization process and therefore the statistical dissipation of the formative time. The lack of vibrational and rotational states of the He atom prevents the shift of the free electron gas spectrum towards lower energies and increases the probability of their capture by SF_6 molecules. Finally, the application of the SF_6/He mixture also has the effect of reducing the greenhouse effect, since the SF_6 gas is one of the most responsible gases for its formation [44, 45].

From fig. 3 it is obvious that the shape of the triggered impulse affects the statistical time. The too fast impulse reduces statistical time but increases its statistical dissipation. It is similar to the too slow impulse. The too-slow impulse increases statistical time, but also increases its statistical dissipation. During the experiments presented in this paper, using a wide range of the triggered impulse rate, the optimal form of the trigger impulse was searched for the operation of the three-electrode spark gaps with minimum statistical dissipation of the trigger time.

As noted, the biggest contribution to the statistical dissipation of the trigger time originates from the statistical dissipation of the statistical time, t_s. In order to reduce it, the concentration of free electrons near the triggered electrode (cathode) should be increased. In addition to that, the experiment was performed with three types of electrodes (the standard triggered electrode, the A type electrode, and the B type electrode, fig. 4 and fig. 9. The idea of applying the electrodes in fig. 9 A type electrode was that its sharp edge (the radius of curvature which tends to zero) would cause a large local increase in the electric field (*i. e.* of critical volume) and cause the cold electrons' emission. The B type electrode of fig. 9, from its side with two such edges, assumed to increase the concentration of cold electrons' emission (and further increase the critical volume), and the cavities located between the sharp edges were intended to provide the additional emission of free electrons by the hollow cathode effect [46, 47]. These cavities in the triggered electrode had diameters greater than the mean electron path length in the applied gas mixture (at a given pressure), and they had been coated with an electron alloy (due to small values of possible output work). In these cavities, an α – radioactive ^{241}Am source was also added during the experiment, for the purpose of increasing the ionization in the cavities (time and the hollow cathode effect).

The experimental procedure was performed in the following steps: 1 – measurement of 1000 values of the trigger time of the dc trigger voltage (voltage rise rate 8 Vs^{-1}, 2 – measuring 1000 values of the trigger times of pulse voltages rates 1 kV(μs)$^{-1}$, kV(μs)$^{-1}$, 10 kV(μs)$^{-1}$,

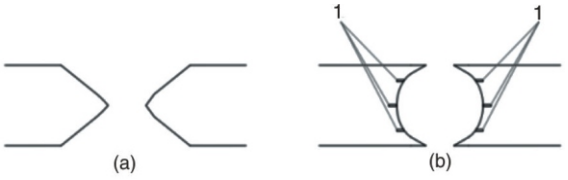

Figure 9. Tested third electrode shapes: *(a) A type and (b) B type; 1 – cavities with or without the ^{241}Am radioactive source*

20 kV(μs)$^{-1}$, 50 kV(μs)$^{-1}$, and 100 kV(μs)$^{-1}$, 3 – measurement of 100 values of the trigger time with variation of the percentage of He in the insulating mixture, 4 – a measurement of 100 values of the trigger time with a variety of trigger electrode types, and 5 – a measurement of 100 values of the trigger time at pressures of 1 bar, 2 bar, 3 bar, 4 bar, 5 bar, and 6 bar. A mixture of $0.8SF_6 + 0.2He$ at a pressure of 4 bar, a 50 kV(μs)$^{-1}$ trigger impulse and a standard triggered electrode were used for all measurements when it was not particularly emphasized. The process of measuring and processing the results was fully automated.

The processing of the results obtained by the experimental procedure included the following steps: 1 – all random variables of the obtained statistical samples were examined according to Chauvenet's criterion, in order to (if possible) reject doubtful measurement results, 2 – all statistical samples of random variables trigger times were tested by applying the χ^2 test and the Kolmogorov test for belonging to the Normal and Weibull distributions; 3 – each statistical sample of 1000 values of a random variable of the trigger time obtained by DC voltages and impulse voltages were divided into 20 chronological sub-statistical samples and tested by *U*-test for belonging to a unique statistical distribution of random samples trigger time of individual statistical samples, and 4 – for statistical samples of 50 random variables obtained by other experiments, the statistical disposal of the random variable was determined by the moment method, depending on the parameters of the experiments under which they were obtained.

RESULTS AND DISCUSSION

As already mentioned, the experimental procedure was performed under well-controlled laboratory conditions. A well-planned and computer-controlled process has produced consistent results. Namely, of all the random variables that have been measured, the trigger time of all experimentally determined statistical samples of Chauvenet's criterion did not detect any result as suspicious and marked for rejection.

Regarding the affiliation of experimentally obtained random variables, the trigger times of all statistical samples of the Normal and Weibull distributions, the obtained results indicate that the tested distributions can be applied equally. More specifically, testing of the experimentally obtained statistical samples showed that about 3 % of the statistical uncertainty belongs to the Weibull distribution, and about 5 % to the Normal distribution. This is a relatively surprising result since the random variables which are characteristic of an electrical breakdown usually belong to the minimum value distributions (Weibull distribution is the most common example) since they cannot be symmetrical by the logic of the observed phenomenon (the gas breakdown).

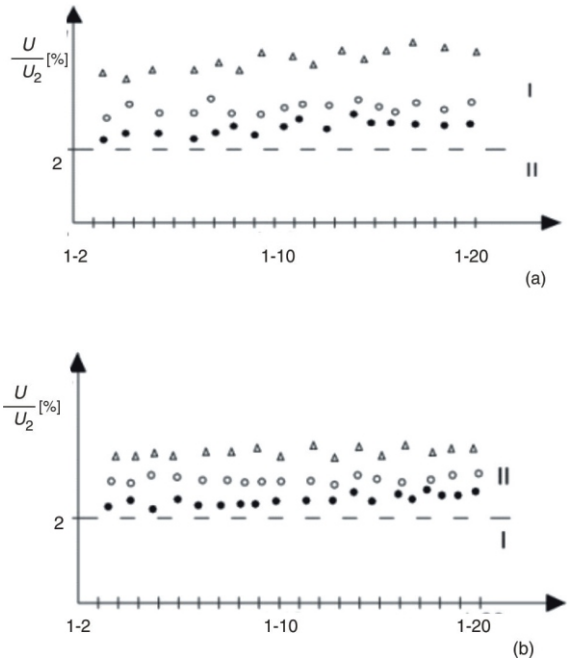

Figure 10. The results of the *U*-test for the affiliation of all random variables with the trigger time of the same statistical sample: *(a) dc triggering and (b) trigger impulse; I – the hypothesis is accepted, II – the hypothesis is rejected*

Figure 10 shows the result of the *U*-test with a statistical uncertainty of 2 % of the statistical sub-samples of a random variable, the breakdown times obtained by dc triggering and trigger impulse. The *U*-test was primarily intended to determine whether all triggers of the three-electrode spark gaps occurred by Mechanism I. Namely, the computer algorithm applied to the experimental designed model of the spark gap was based on dc breakdown mechanisms. However, in reality, the trigger mechanism is exerted by an impulse voltage. Since the value of the dc breakdown voltage is a deterministic magnitude and the value of the impulse breakdown voltage is stochastic, it could be expected that in the case of impulse triggering, sometimes a deviation from the triggering of Mechanism I would occur. The results which are shown in fig. 10 and the sizes of the tested sample confirm (with a statistical uncertainty, the order of the size of per mille) the justification of the applied design method of the three-electrode spark gaps.

Figure 11 shows the effect of the percentage of He in the insulating mixture on the mean value and the statistical dissipation of the random value of the trigger time, obtained at a pressure of the mixture of 4 bars by a spark gap with a standard electrode. It is obvious from fig. 11 that the mean of the triggered voltage and the statistical dissipation of the trigger time decreases with an increasing percentage of the mixture. This effect is stabilized for a percentage composition of He about 20 %. The further increasing of the percentage composition does not reduce the significant statistical

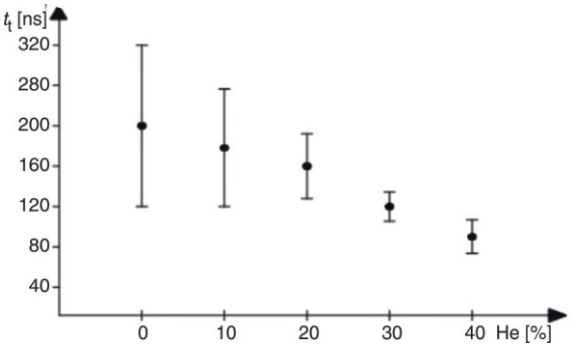

Figure 11. The influence of the percentage of He in the mixture on the mean of the statistical dissipation of the trigger time; rise rate of 50 kV(μs)$^{-1}$, standard trigger electrode

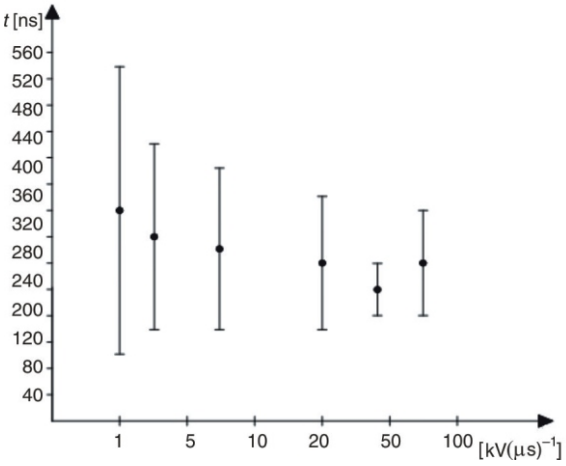

Figure 12. The influence of the trigger impulse rate on the mean value of the statistical dissipation of the trigger time; mixture of 0.8 SF_6 + 0.2 He, standard triggered electrode

dissipation of the random variable of the trigger time, but decreases the value of the voltage breakdown. For this reason, and considering both the economic aspects and the sustainability of the composition of the mixture for a long time, 0.8SF_6 + 0.2He proved to be the optimal percentage composition of the mixture.

Figure 12 shows the statistical deviations of the random variable obtained by applying different trigger impulse rates. A standard trigger electrode was used. Based on fig. 12 it can be concluded that the least statistical dissipation of the random magnitude of the trigger time is the one obtained by impulses of the velocity of 50 kV(μs)$^{-1}$.

Figure 13 shows the influence of the triggered electrode shape on the mean value and the statistical dissipation of the random variable of the trigger time. It is also obvious from fig. 13 that the least statistical dissipation of the random variable is when the B-type trigger electrode whose cavities contain a small amount of ^{241}Am is applied. In case the cavity of the triggered electrode is only alloyed with an electron, the statistical dissipation of the random variable of the trigger time is

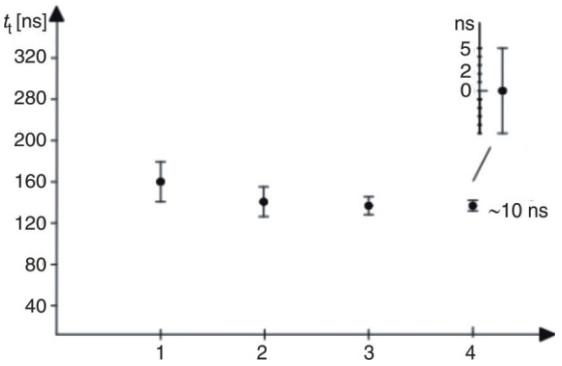

Figure 13. The influence of the triggered electrode shape on the mean value and the statistical dissipation of the trigger time; mixture of 0.8 SF_6 + 0.2 He, rise rate of 50 kV(μs)$^{-1}$; 1 – the standard third electrode, 2 – the third electrode type A, 3 – the third type B electrode with no radioactive source, 4 – the third type B electrode with a radioactive source

slightly higher (but with the ecological advantage of unused radioactive sources). Figure 13 also clearly shows the synergy of the influences of all the effects tested on the random variable. It is positive. The statistical dissipation of the random magnitude of the trigger time is the breakdown time in the case of the *B*-type electrode with cavities containing a small amount of ^{241}Am triggered by an impulse of 50 kV(μs)$^{-1}$ about 5 ns.

Figure 13 The influence of the triggered electrode shape on the mean value and the statistical dissipation of the trigger time; mixture of 0.8SF_6 + 0.2He, rise rate of 50 kV(μs)$^{-1}$; 1 – the standard third electrode, 2 – the third electrode A-type, and 3 – the third B-type electrode with no radioactive source, 4 – the third B-type electrode with a radioactive source

It should be mentioned here that the application of different pressures, 1 bar, 2 bar, 3 bar, 4 bar, 5 bar, and 6 bar, did not affect the results, *i. e.* identical results were obtained.

CONCLUSION

Owing to new solutions applied for the construction of the three-electrode spark gaps with a separate triggered electrode, the statistical dissipation of the random trigger time variable that accomplish the requirements of high-energy physics (*i. e.* located in the sub-microsecond field) have been obtained. This is mainly due to the computer designed solution, which allows only one, optimal trigger mechanism. Furthermore, the application of a mixture of SF_6 and He contributed to increasing in a number of free (initial electrons potentially) since He readily rejects one electron and does not slow down the spectrum of the free electron gas by arousing the vibrational and rotational quantum mechanical states of its atom (thereby increasing the probability of producing negative SF6 ions). The increasing number of free electrons, especially in the critical volume, is contributed by the third electrode with a double-ionization process. The

increase in the number of free electrons significantly contributes to the decrease in the statistical dissipation of the statistical time, which contributes most to the statistical dissipation of the trigger time. With its presence, gas He also helps to reduce the statistical dissipation of the formative time as it accelerates the thermo-ionization process with its small molecule. It is important to point out that experiments at different pressures have shown that the results obtained are not dependent on the pressure. This indicates that the optimal construction solution obtained in the reduced model, can be transferred to the enlarged prototype according to the law of similarity without taking, as a geometric parameter, the mean free path length of the electron (which is often a limitation for the application of the law of similarity).

ACKNOWLEDGMENT

This work was supported by the Ministry of Education, Science and Technological Development the Republic of Serbia under contract no. 171007.

REFERENCES

[1] Vries, L. M. J., Damstra, G. C, Triggered Vacuum Gaps in a High Power Three-Phase Synthetic Test Circuit, *IEEE Transactions on Dielectrics and Electrical Insulation, 20* (1985), 4, pp. 755-758
[2] Kugler, R., Thermal and Dynamic Short-Circuit Demands in High-Voltage Power Switches, *Elektrotechnik und Maschinenbau, 102* (1985), 7-8, pp. 298-304
[3] Osmokrović, P., Rasović, K., Optimization of the Three-Electrode Spark Gap Characteristics, Eighth IEEE International Conference on Pulsed Power, 1991, pp. 859-862
[4] Hancox, R., Low-Pressure Gas Discharge Switches for Use in Fusion Experiments, *Proceedings*, *Institution of Electrical Engineers, 111* (1964), 1, pp. 203-213
[5] Tian, Z. X., High Voltage Triggered Spark Gap with Repeatable Gas Filling Structure, *Applied Mechanics and Materials, 432* (2013), pp. 373-377
[6] Osmokrovic, P., *et al*., Triggered Three-Electrode Spark Gaps, Digest of Technical Papers, IEEE International Pulsed Power Conference, 1995, pp. 822-827
[7] Osmokrović, P., *et al*., Reliability of Three-Electrode Spark Gaps, *Plasma Devices Operations, 16* (2008), 4, pp. 235-245
[8] Osmokrović, P., Arsić, N., Application of Vacuum Three-Electrode Spark Gaps for Synthetic Circuits, The International Symposium on Discharge and Electrical Insulation in Vacuum (ISDEIV), 1992, pp. 624-628
[9] Sullivan, D. L., *et al*., Study of Laser Target Triggering for Spark Gap Switches, *IEEE Transactions on Dielectrics and Electrical Insulation, 16* (2009), 4, pp. 956-960
[10] Forestier B., *et al*, Triggering, Guiding and Deviation of Long Air Spark Discharges with Femtosecond Laser Filament, *AIP Advances, 2* (2012), 1, pp. 012151-13
[11] Guenther, A. H., Bettis, J. R., The Laser Triggering of High-Voltage Switches, *Journal of Applied Physics, 11* (1978), pp. 1577-1613
[12] Rahaman H., *et al*., Design of a SF6-Gas-Filled Spark Gap Switch for High-Voltage Application, *IEEE Transactions on Plasma Science, 38* (2010), 10, pp. 2758-2763
[13] Yin, J., *et al*., 2.8-MV Low-Inductance Low-Jitter Electrical-Triggered Gas Switch, *IEEE Transactions on Plasma Science, 44* (2016), 10, pp. 2045-2052
[14] Osmokrović, P., *et al*., Triggered Vacuum and Gas Spark Gaps, *IEEE Transactions on Power Delivery, 11* (1996), 2, pp. 858-864
[15] Von Angel, A., Ionized Gases, *Physics Today, 17* (1964), 9, pp. 108-108
[16] Osmokrović, P., *et al*., Mechanism of Electrical Breakdown of Gases for Pressures from 10-9 to 1 bar and Inter-Electrode Gaps from 0.1 to 0.5 mm, *Plasma Sources Science and Technology, 16* (2007), 3, pp. 643-655
[17] Dekić, S., *et al*., Conditions for the Applicability of the Geometrical Similarity Law to Impulse Breakdown in Gases, *IEEE Transactions on Dielectrics and Electrical Insulation, 17* (2010), 4, pp. 1185-1195
[18] Polužanski, V. S., *et al*., Computer Non-Iterative Data Acquisition of Particle, *Nucl Technol Radiat, 34* (2019), 1, pp. 65-71
[19] Larsson, A., Gas-Discharge Closing Switches and Their Time Jitter, *IEEE Transactions on Plasma Science, 40* (2012), 10, pp. 2431-2442
[20] Tie, W., *et al*., A Novel Low-Jitter Plasma-Jet Triggered Gas Switch Operated at a Low Working Coefficient, *Review of Scientific Instruments, 85* (2014), no. 2, pp. 023504-5
[21] Obrenović, M. D., *et al*., Statistical Review of the Insulation Capacity of the Geiger-Mueller Counter, *Nucl Technol Radiat, 33* (2018), 4, pp. 36-374
[22] Pejović, M. M., *et al*., Investigation of Breakdown Voltage and Electrical Breakdown Time Delay in Air-Filled Tube in Presence of Combined Gas and Vacuum Breakdown Mechanism, *Vacuum, 86* (2012), 12, pp. 1860-1866
[23] Radmilović-Radjenović, M. D., *et al*., The Effect of Enhanced Field Emission on Characteristics of Super Conducting Radio Frequency Cavities, *Nucl Technol Radiat, 33* (2018), 4, pp. 341-346
[24] Osmokrović, P., *et al*., Determination of Pulse Tolerable Voltage in Gas-Insulated Systems, *Japanese Journal of Applied Physics, 47* (2008), 12, pp. 8928-8934
[25] Raizer, Y. P., Gas Discharge Physics, Springer-Verlag Berlin Heidelberg, Germany, 1991
[26] Pejović, M. M., *et al*., Kinetics of Positive Ions and Electrically Neutral Active Particles in Afterglow in Neon at Low Pressure, *Physics of Plasmas, 21* (2014), 4, pp. 042111-8
[27] Jusić, A., *et al*., Synergy of Radioactive ^{241}Am and the Effect of Hollow Cathode in Optimizing Gas-Insulated Surge Arresters Characteristics, *Nucl Technol Radiat, 33* (2018), 3, pp. 260-267
[28] Pejovic, M. M., *et al.*, Investigation of Post-Discharge Processes in Nitrogen at Low Pressure, *Physics of Plasmas, 19* (2012), 12, pp. 123512-8
[29] Dolićanin, E., Fetahović, I. S., Monte Carlo Optimization of Redundancy of Nanotechnology Computer Memories in the Conditions of Background Radiation, *Nucl Technol Radiat, 33* (2018), 2, pp. 208-216
[30] Morghen, D., Untersuchung Uber die Zundung Einer Grossen Anzal Parallelgeschalter Dreielectroden Funkentrecken, *ETZ-A, 88* (1967), pp. 480-487
[31] Li, L., *et al*., Modeling of Switching Delay in Gas-Insulated Trigatron Spark Gaps, *Journal of Applied Physics, 111* (2012), 5
[32] Woodworth, J. R., *et al*., Low-Inductance Gas Switches for Linear Transformer Drivers, *Physical Review Accelerators and Beams, 12* (2009), 6, pp. 060401-060418

[33] Beyer, M., *et al*., Hochspannungtechnik: Theoretische und Praktische Grundlagen, Springer-Verlag, Berlin Heidelberg, 1986
[34] Pejović, M., *et al*., Processes in Insulating Gas Induced by Electrical Breakdown Responsible for Commercial Gas-Filled Surge Arresters Delay Response, *Vacuum, 137* (2017), pp. 85-91
[35] Chen, L., *et al*., Study on a Plasma-Jet Triggered Trigatron Switch in a 1.0 MJ-Flashlamp Driven Power System, *Journal of Fusion Energy, 35* (2016), 2, pp. 240-243
[36] Rajović, Z., et al., Influence of SF_6-N2 Gas Mixture Parameters on the Effective Breakdown Temperature of the Free Electron Gas, *IEEE Transactions on Plasma Science, 41* (2013), 12, pp. 3659-3665
[37] Osmokrović, P., *et al*., Model Law for Gas Isolated System, *IEEE Transactions on Plasma Science, 28* (2000), 1, pp. 298-302
[38] Brown, S. C., Holt, E. H., Introduction to Electrical Discharges in Gases, *American Journal of Physics, 36* (1968), 9, pp. 854-854
[39] Perazić, L. S., *et al*., Application of an Electronegative Gas as a Third Component of the Working gas in the Geiger-Muller Counter, *Nucl Technol Radiat, 33* (2018), 3, pp. 268-274
[40] Osmokrović, P., *et al*., Measuring Probe for Fast Transients Monitoring in Gas Insulated Substation, *IEEE Transactions on Instrumentation and Measurement, 46* (1997), 1, pp. 36-44
[41] ***, BIPM, IEC, IFCC, ISO, IUPAC, IUPAP and OIML: Guide to the Expression of Uncertainty in Measurement, Geneva, Switzerland: International Organization for Standardization, 1995
[42] Stanković, K., Vujisić, M., Influence of Radiation Energy and Angle of Incidence on the Uncertainty in Measurements by GM Counters, *Nucl Technol Radiat, 23* (2008), 1, pp. 41-42
[43] Vulević, B., Osmokrović, P., Evaluation of Uncertainty in the Measurement of Environmental Electromagnetic Fields, *Radiation Protection Dosimetry, 141* (2010), 2, pp. 173-7
[44] Arsić, N., Osmokrović, P., Influence of the Gas Insulation Parameters on the Three-Electrode Spark Gap Functioning, The International Symposium on Discharge and Electrical Insulation in Vacuum (ISDEIV), 1996, pp. 77-80
[45] Warne, L. K., *et al*., Criterion for Spark-Breakdown in Non-Uniform Fields, *Journal of Applied Physics, 115* (2014), 14, pp. 143303-8
[46] Dekić. S., *et al*., Conditions for the Applicability of the Geometrical Similarity Law to Impulse Breakdown in Gases, *IEEE Transactions on Dielectrics and Electrical Insulation, 17* (2010), 4, pp. 1185-1195
[47] Osmokrović, P., *et al*., Numerical and Experimental Design of Three-Electrode Spark Gap for Synthetic Test Circuits, *IEEE Transactions on Power Delivery,* 9 (1994), 3, pp. 1444-1450

Received on July 6, 2021
Accepted on November 8, 2021

**Теодора М. НЕДИЋ, Ђорђе Р. ЛАЗАРЕВИЋ,
Ковиљка Ћ. СТАНКОВИЋ, Ненад М. КАРТАЛОВИЋ**

ОПТИМИЗАЦИЈА БРЗИХ ТРОЕЛЕКТРОДНИХ ИСКРИШТА ИЗОЛОВАНИХ СМЕШОМ SF_6 И He

У овом раду разматрана је могућност смањења расипања окидног времена троелектродног искрштa са издвојеном окидном електродом. Рад је теоријске, нумеричке и експерименталне природе. Експерименти су рађени на моделу искришта под добро контролисаним лабораторијским условима. Доказано је да се резултати добијени на моделу могу применити на прототип искришта. За разлику од досадашњих истраживања у овој области, коришћено је компјутерски дизајнирано искриште које може бити окинуто само једним механизмом. Такође су, у односу на претходна истраживања, коришћене смеше гасова SF_6 и He као и треће електроде са двоструким јонизационим ефектом. Добијени резултати су показали да оптимална комбинација конструкционог решења, изолационог гаса, окидног импулса и облика окидне електроде смањују стохастичко расипање случајне променљиве далеко у суб микросекундну област. Овај резултат је од велике важности за паралелно окидање струјних и напонских генератора у циљу суперпозиције сигнала.

Кључне речи: троелектродно искриште, статистичко расипање времена окидања, смеша гасова SF_6 и He